MAGNETO-OPTICAL MEASUREMENTS OF THE LIFETIME SPECTRUM OF TRANSIENT VORTEX STATES IN BSCCO

B. Kalisky[1], A. Shaulov[1], T. Tamegai[2] and Y. Yeshurun[1]
1. Institute of Superconductivity, Department of Physics, Bar-Ilan University, Ramat-Gan 52900, Israel
2. Department of Applied Physics, The University of Tokyo, Hongo, Bunkyo-ku, Tokyo 113-8656, Japan

Abstract:

We employ a high-speed magneto-optical system to image the processes of creation and annealing of transient disordered vortex states and utilize these data to measure the lifetime, τ, of these states as a function of induction B and temperature T. τ increases monotonically with B and diverges as B approaches the vortex order-disorder transition induction. An exponential increase of τ is obtained as temperature is lowered. The *same* τ(B,T) curves are obtained, independent of the way the transient states were prepared.

Key words: Vortex phase transitions; transient vortex state; second magnetization peak

Recent studies of the vortex phase diagram in $Bi_2Sr_2CaCu_2O_{8+\delta}$ (BSCCO) have shown that the disorder-driven vortex phase transition is obscured by transient disordered vortex states (TDVS) [1-9], created by edge contamination during field ascending [1, 2] or by "supercooling" of the disordered vortex lattice during field descending [4, 8]. Knowledge of the lifetime spectrum τ of these transient states as a function of induction, B, and temperature, T, is required to reveal the underlying thermodynamic order-disorder phase transition [10, 11]. In this paper we employ a high-speed magneto-optical system to image the processes of creation and annealing of TDVS and utilize these data to directly measure the lifetime τ(B,T) in three different experiments: (i) Continuous injection of transient vortex states

while ramping up the external magnetic field, (ii) Annealing of injected transient states while keeping the external field constant, and (iii) Annealing of transient 'supercooled' disordered states while ramping down the external field.

Measurements were performed on a 1.55×1.25×0.05 mm³ $Bi_2Sr_2CaCu_2O_{8+\delta}$ single crystal ($T_c \sim 92$ K). The crystal was grown using the traveling solvent floating zone method [12]. This crystal was specially selected for its uniformity of flux penetration and was checked by magneto-optical imaging before and after it was cut into a rectangle. In the course of measurements, magneto optical (MO) snapshots of the induction distribution across the sample surface were recorded at time intervals of typically 40 ms, using iron-garnet MO indicator with in-plane anisotropy [13] and a high speed CCD camera (Hamamatsu C4880-80).

In the first experiment, referred to as *Field Sweep Up (FSU)* experiment, the sample was cooled down to the measuring temperature in zero field, then the external magnetic field, H_{ext}, was ramped up at a constant rate between 4 and 1600 G/sec, from zero to about 850 G. While the external magnetic field was ramped up, snapshots of the induction distribution across the crystal surface were taken successively at constant field intervals (usually 10 G).

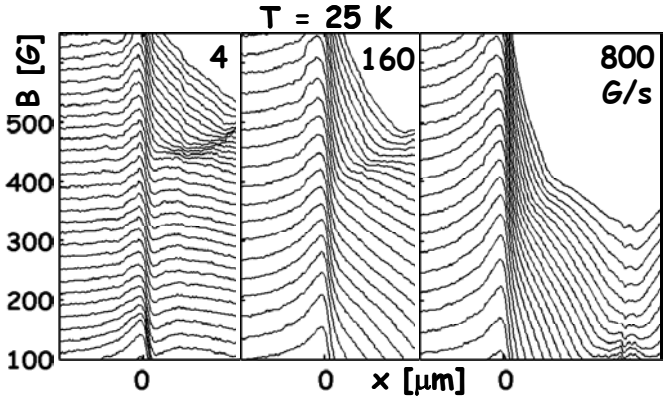

Figure 1. Induction profiles measured at T= 25 K while ramping the external field at different rates. As dH_{ext}/dt increases, the first break in the profiles appears at a lower induction.

Figure 1 shows the induction profiles across the crystal width deduced from the magneto-optical images measured at T= 25 K, while the external field was ramped up at a rate of 4, 160, and 800 G/sec. A sharp change in the slope of the profile ("break") appears near the edge at B_{f0} = 450, 400, and 330 G, respectively, indicating coexistence of two distinct vortex states, characterized by high persistent current state near the sample edges and a low persistent current state near the center [3]. The high persistent current

state is identified as a TDVS, because it decays with time when the external field is kept constant (see annealing experiment described below). When the external field is continuously increased, the break moves towards the sample center, indicating propagation of the transient disordered state front deeper into the sample. At the same time, the induction at the break increases monotonically with a rate decreasing with time.

These results can be explained in terms of competition between injection and annealing processes of TDVS. While the rate of injection remains approximately constant, the rate of annealing is high for low inductions, and decreases sharply as the induction increases towards B_{od}. The first appearance of the break, at B_{f0}, indicates a stage where the injection rate starts to overcome the annealing rate. The injection rate is determined by dH_{ext}/dt while the annealing rate is determined by $1/(d\tau/dB)$ [14]. Thus, at $B = B_{f0}$,

$$\left(\frac{\partial \tau}{\partial B}\right)_{B=B_{f0}} = \frac{1}{dH_{ext}/dt}. \quad (1)$$

Based on this equation, one can determine τ *vs.* B by measuring the induction B_{f0} for different rates of external magnetic field sweep. The circles in Figure 2 describe the extracted values of $\tau(B)$ from FSU experiments at 23 K. Evidently, τ increases monotonically with the induction and exhibits a sharp increase as the thermodynamic order-disorder transition field, B_{od}, is approached.

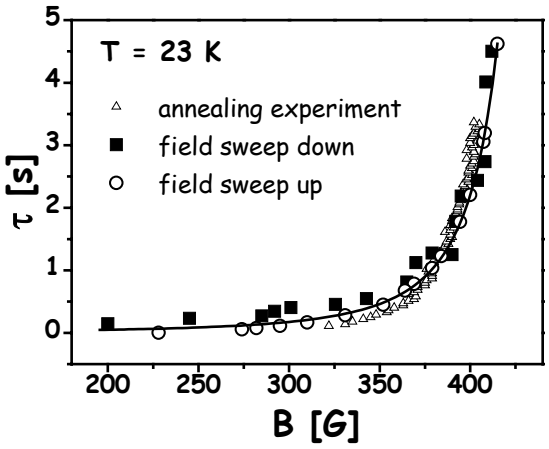

Figure 2. Measurements of the annealing time τ as a function of B from field sweep up (circles), field sweep down (squares) and annealing (triangles) experiments. The solid line is a fit to Eq. 3.

In the second experiment, referred to as *annealing* experiment, injection of TDVS throughout the sample was accomplished by abruptly raising the external field to a target value between 140 and 850 G (rise-time < 50 ms). Immediately after reaching the target value of the external field, magneto-optical snapshots of the induction distribution across the sample surface were recorded at time intervals of 40 ms for 4 seconds, and 300 ms for additional 26 seconds.

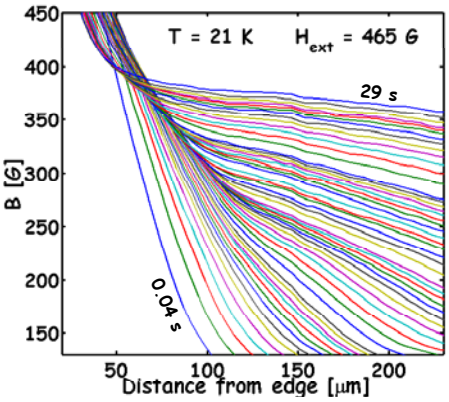

Figure 3. Time evolution of the induction profiles after abruptly increasing the external field from zero to 465 G. At approximately t = 0.5 s, a sharp change (a 'break') in the slope of the profiles appears, progressing with time towards the sample edge.

Figure 3 shows the time evolution of the induction profiles at T= 21 K after abruptly increasing the external field from zero to 465 G. Initially, the profiles are smooth, without a break, indicating a single vortex phase throughout the sample. However, after approximately 0.5 second, a break appears in the slope of the induction profiles, progressing with time towards the sample edge. The break separates between a high persistent current state near the sample edge and a low persistent current state near the center. The high persistent current region near the edge shrinks with time, and therefore the vortex state in this region is identified as a transient disordered state. The vortex state in the expanding, low persistent current region near the center, is identified as the thermodynamic quasi-ordered phase [3].

The lifetime, τ, can be measured directly in annealing experiments at constant field by employing the following procedure. From the MO profiles we extract local $j \sim dB/dx$ at different times for all measured external fields, and plot it versus local B. Typical results, measured at 21 K, are presented in Figure 4 for $x_0 = 110$ μm measured from the sample edge. In the figure, data points corresponding to different times are marked by different symbols, and the solid lines connect all points measured at the same indicated time. Each curve may be considered as an instantaneous local magnetization curve, and

the set of curves demonstrates the time evolution of the second magnetization peak (SMP): At short times ($t < 0.5$ s), no SMP is observed. A trace of a SMP first appears at $t \sim 0.52$ s, and it continues to develop with time, while its onset shifts to higher inductions (from 200 G at 0.52 s to 360 G at 29 s).

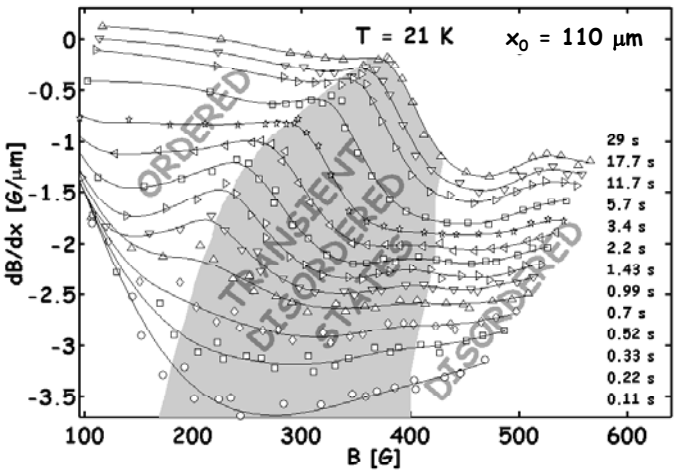

Figure 4. Typical $dB/dx \sim j$ vs. local B at $x_0 = 110$ μm for the indicated times, measured at 21 K. Grey area marks the transient state zone.

In figure 4 we mark three zones corresponding to quasi-ordered, disordered and TDVS. The identification of these zones is done directly from the local data as described elsewhere [11, 15]. The most intriguing observation in figure 4 is that the left border of the transient vortex state zone is marked by the onset of the SMP. In the region to the left of this zone, the transient disordered state has been annealed and a thermodynamic quasi-ordered phase has been established. In the region to the right of this zone, a thermodynamic disordered vortex phase has been established.

From the instantaneous magnetization curves depicted in figure 4, one can directly measure τ as a function of the local induction B. By definition, τ is the time elapse between the onset of the external field and the moment when the transient state at x_0 disappears. We argue that the time corresponding to each instantaneous curve is the annealing time of the initial transient vortex state generated at the induction, B_{on}, corresponding to the SMP onset. This is because for inductions smaller than B_{on} the vortices are already in a quasi-ordered phase, and for inductions just above B_{on} vortices are still in a transient disordered state. The triangles in figure 2 show τ as a function of B measured in this way for T = 23 K.

In the third experiment, referred to as *Field Sweep Down (FSD)* experiment, the TDVS were generated by "supercooling" of the disordered vortex state. In this experiment, an external field of 850 G was initially applied for long enough time to ensure establishment of a disordered vortex phase. The field was then ramped down to zero at a constant rate between 4 and 1600 G/sec. While the external field was ramped down, snapshots of the induction distribution across the crystal surface were taken successively at constant field intervals (usually 10 G).

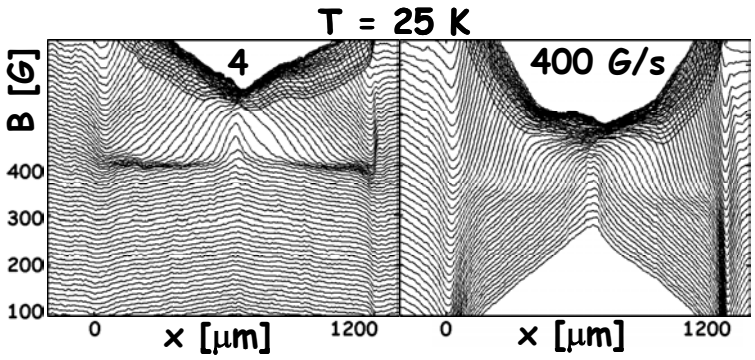

Figure 5. Induction profiles measured at T= 25 K while ramping down the external field at different rates. As $dH_{ext}/dt|$ increases, the breaks in the profiles appear at lower inductions.

Figure 5 shows the induction profiles taken at T= 25 K, while the external field was ramped down at rates of 4 and 400 G/sec. The profiles exhibit a break, progressing into the sample interior with time. In contrast to FSU experiments, here the breaks appear at approximately the same induction, $B_f \approx B_{f0}$ = 400 and 350 G, respectively, almost independent of the location in the sample. The breaks reveal coexistence of a quasi-ordered vortex phase (characterized by low persistent current density) near the sample edges, and a TDVS (characterized by high persistent current density), in the sample interior.

In this experiment, transient states are created when crossing B_{od}, and are dragged down to B_{f0} during a time $t \approx \tau(B_{f0})$. Thus,

$$\tau(B_{f0}) = \frac{B_{od} - B_{f0}}{\left|dH_{ext}/dt\right|} \qquad (2)$$

The squares in figure 2 describe the extracted values of $\tau(B)$ from FSD experiments, using B_{od} of 460 G.

Looking back at Figure 2, we can draw two important conclusions. First, the values of $\tau(B)$ extracted from the above three experiments yield the

same curve, *independent* of the way the TDVS was prepared. Second, as expected, τ diverges as B approaches the transition induction B_{od}. The data points may be fitted to

$$\tau = \tau_0/(1-B/B_{od})^{\gamma} \quad (3)$$

The fit (described by the solid line in the figure) yields $\tau_0 = 0.011$ s, $\gamma = 2.6$ and $B_{od} = 460$ G.

Measurements of τ (B) at different temperatures show that the lifetime spectrum of the TDVS widens as temperature is lowered [10]. Fits of these data to Eq. 3, yields τ_0(T), which apparently increases exponentially as the temperature is lowered [14]. The exponential increase of τ(B) with decreasing temperature, explains the broadening of the second magnetization peak and its disappearance below a certain temperature [10, 11, 16-21] - a phenomenon that was misinterpreted as a termination of the transition line.

From all the above, it is apparent that TDVS are involved in any direct measurement of the thermodynamic order-disorder transition line, B_{od}(T). However, indirect measurements of B_{od}(T) may be obtained by fitting τ(B) to Eq. 3 at various temperatures. Measurement of the transition line in this method yields results which are significantly different from the non-equilibrium transition lines, commonly measured from the onset of the second magnetization peak, neglecting effects of transient vortex states.

Acknowledgments: We acknowledge support from the German-Israel Foundation (GIF). Y.Y. acknowledges support from the ISF Center of Excellence Program, and by the Heinrich Hertz Minerva Center for High Temperature Superconductivity.

1. Y. Paltiel, E. Zeldov, Y. Myasoedov, M.L. Rappaport, G. Jung, S. Bhattacharya, M.J. Higgins, Z.L. Xiao, E.Y. Andrei, P.L. Gammel, and D.J. Bishop, Phys. Rev. Lett. **85**, 3712 (2000).
2. Y. Paltiel, E. Zeldov, Y.N. Myasoedov, H. Shtrikman, S. Bhattacharya, M.J. Higgins, Z.L. Xiao, E.Y. Andrei, P.L. Gammel, and D.J. Bishop, Nature **403**, 398 (2000).
3. D. Giller, A. Shaulov, T. Tamegai, and Y. Yeshurun, Phys. Rev. Lett. **84**, 3698 (2000).
4. C.J. van der Beek, S. Colson, M.V. Indenbom, and M. Konczykowski, Phys. Rev. Lett **84**, 4196 (2000).
5. H. Kupfer, A. Will, R. Meier-Hirmer, T. Wolf, and A.A. Zhukov, Phys. Rev. B **63**, 214521 (2001).
6. M. Konczykowski, C.J. van der Beek, S. Colson, M.V. Indenbom, P.H. Kes, Y. Paltiel, and E. Zeldov, Physica C **341**, 1317 (2000).
7. D. Giller, B. Kalisky, A. Shaulov, T. Tamegai, and Y. Yeshurun, J. Appl. Phys. **89**, 7481 (2001).

8. D. Giller, A. Shaulov, L. Dorosinskii, T. Tamegai, and Y. Yeshurun, Physica C **341**, 987 (2000).
9. E.Y. Andrei, Z.L. Xiao, W. Henderson, Y. Paltiel, E. Zeldov, M. Higgins, S. Bhattacharya, P. Shuk, and M. Greenblatt, Condensed Matter Theories **16**, 241 (2001).
10. B. Kalisky, D. Giller, A. Shaulov, and Y. Yeshurun, Phys. Rev. B **67**, R140508 (2003).
11. B. Kalisky, A. Shaulov, and Y. Yeshurun, Phys. Rev. B **68**, 012502 (2003).
12. N. Motohira, K. Kuwahara, T. Hasegawa, K. Kishio, and K. Kitazawa, Journal of the Ceramic Society of Japan **97**, 1009 (1989).
13. V.K. Vlasko-Vlasov and *e. al.*, in *Physics and Materials Science of Vortex States, Flux Pinning and Dynamics*, R. Kossowski and *e. al.*, NATO ASI: Kluwer, Kordrecht. p. 205. (1999).
14. B. Kalisky, Y. Bruckental, A. Shaulov, and Y. Yeshurun, Unpublished.
15. B. Kalisky, A. Shaulov, T. Tamegai, and Y. Yeshurun, J. Appl. Phys. **93**, 8659 (2003).
16. Y. Yeshurun, N. Bontemps, L. Burlachkov, and A. Kapitulnik, Phys. Rev. B **49**, 1548 (1994).
17. S.L. Li and H.H. Wen, Phys. Rev. B **65**, 214515 (2002).
18. Y. Yamaguchi, G. Rajaram, N. Shirakawa, A. Mumtaz, H. Obara, T. Nakagawa, and H. Bando, Phys. Rev. B **63**, 014504/1 (2000).
19. T. Tamegai, Y. Iye, I. Oguro, and K. Kishio, Physica C **213**, 33 (1993).
20. M.F. Goffman, J.A. Herbsommer, F. de la Cruz, T.W. Li, and P.H. Kes, Phys. Rev. B **57**, 3663 (1998).
21. S. Anders, R. Parthasarathy, H.M. Jaeger, P. Guptasarma, D.G. Hinks, and R. van Veen, Phys. Rev. B **58**, 6639 (1998).